NUCLEAR INSTRUMENTS AND METHODS 135 (1976) 151–156; © NORTH-HOLLAND PUBLISHING CO.

PRODUCTION AND TRANSPORT OF CONDUCTION ELECTRONS IN A LIQUID ARGON IONIZATION CHAMBER

W. HOFMANN, U KLEIN, M. SCHULZ, J SPENGLER and D. WEGENER

Institut fur Experimentelle Kernphysik der Universität (TH) und des Kernforschungszentrums Karlsruhe, Karlsruhe, W. Germany

Received 27 February 1976

Free electrons produced by α- and β-particles in a liquid argon ionization chamber have been detected. For minimum ionizing particles the collected charge saturates at a field strength of $E \lesssim 15$ kV/cm $(95 \pm 4)\%$ of the produced electrons were collected. For strongly ionizing α-particles no saturation was observed up to a field strength of 40 kV/cm, where $(25 \pm 3)\%$ of the produced electrons were detected. The influence of oxygen and nitrogen, solved in the liquid argon, on the charge collection was studied. A nonlinear relationship between the mean free path length for absorption and the applied electric field indicates the existence of hot electrons in liquid argon. The recombination effect in the ionization column produced by α-particles is enhanced by oxygen and nitrogen impurities in liquid argon.

1. Introduction

Shower counters are of increasing importance for the identification and energy determination of elementary particles[1]). Iron–scintillator respectively lead–scintillator sandwich counters represent the classical version of this detector[2]). Following a proposal of Willis[3]) liquid argon has been used as the detector material sandwiched between metallic electrodes, where the charge produced by the ionizing shower in the liquid is collected[3–6]). Compared to other sampling detectors the liquid argon chamber has several important advantages: simple and reliable absolute calibration with a test pulser is possible, the detector shows good homogeneity over the whole volume, different kinds of particles of the same energy have approximately the same pulse height and it is feasible to study the details of the shower development in lateral[10]) and longitudinal direction[7]).

For a quantitative interpretation of the data collected with a liquid argon sampling shower counter a quantitative understanding of the recombination effects of the Ar^+-ions and the free electrons, produced by the shower particles, is necessary[4,8]). Moreover the influence of oxygen and nitrogen impurities on the charge collection efficiency has to be known, if one wants to build a detector lay-out which guarantees stable working conditions.

In this paper we report on measurements performed with an α-source and a β-source in a single cell liquid argon ionization chamber. The experiment aimed to collect information relevant in the context of questions mentioned above. The outline is the following: in section 2 we describe the set-up used and discuss the calibration procedure. In section 3 the results of the measurements are presented, which are discussed and compared to other experiments in section 4.

2. Apparatus

The ionization chamber for the detection of β-particles[9]) was installed in a dewar vessel of 35 cm diameter and 75 cm height. The dewar was filled with liquid argon, which was indirectly cooled by liquid nitrogen flowing through a copper pipe placed at the top of the vessel.

Before filling, the dewar was evacuated to a pressure of 10^{-3} torr and then flushed with clean argon gas. This procedure was repeated a few times. Pure liquid argon* ($PO_2 \leq 1$ ppm, $PN_2 \leq 4$ ppm) was used to fill the dewar. In order to increase the concentration of oxygen respectively nitrogen impurities in the liquid argon by definite amounts, a defined mixture of pure argon gas and oxygen respectively nitrogen was added to the gas phase at the top of the dewar vessel. After the equilibrium between the gas and the liquid was established, the concentration of the impurities in the gas phase was measured using a gas-chromatograph †. The measurements have been corrected for the different concentrations of the impurities in the liquid and in the gaseous phase using Henry's law[10]).

The ionization chamber, shown in fig. 1, consists of two 50 μm thick copper electrodes, whose distance D could be varied by support rings in the range $2\ \text{mm} \leq D \leq 4$ mm. The cathode was connected to a pream-

* Messer Griesheim, Ludwigsburg.
† AL8, Tres Bas Temperature.

plifier. The high voltage applied to the anode could be varied between 0 kV and 4 kV. Outside of the ionization chamber a $^{90}Sr+^{90}Y$ β-source was placed at a distance of 0.5 mm from the anode. The β-source and the anode were dc coupled. A scintillation counter was placed 3 mm behind the cathode. This set-up allowed to record only charge pulses produced by β-particles which traversed the liquid argon ionization chamber. Due to a proper chosen discriminator level for the pulse heights of the scintillation counter, only β-particles with an energy greater than 700 keV at the end of the ionization chamber were detected. Hence the energy loss in the ionization chamber was constant[11])

$$\frac{dE}{dx} = 1.9 \text{ MeV/cm} . \quad (1)$$

The source strength of the β-source was 10^3 decays/(s cm^2), therefore polarization effects are negligible in the present experiment.

The pulses of the ionization chamber were amplified, shaped and recorded by a multichannel analyzer, which was gated by the scintillation counter pulse. The typical noise contribution to the signal was 0.5 fC fwhm. The ionization chamber was calibrated with a pulse generator whose pulse shape was adapted carefully to that of the ionization chamber pulses.

The systematic errors of the detected charges are due to calibration errors ($\pm 5\%$) and errors of the pulse height determination, which varied between $\pm 5\%$ at small pulse heights and $\pm 1\%$ at large ones. The distance between the electrodes was determined with a precision of $\pm 5\%$.

As sources for strongly ionizing particles α-sources of ^{241}Am and ^{210}Po of 0.3 μC strength have been used[10]). They were deposited on an area of 3 cm^2, hence polarization effects due to Ar^+ ions are negligible. The charge pulses have been recorded with a multichannel analyzer, no gate signal was available. The gap width of the ionization chamber was 1.5 mm respectively 2 mm for the two α-sources. A typical α-line is shown in fig. 2. A slight asymmetry is due to the finite thickness of the source as proven by the full line included into fig. 2, which is derived from the energy spectrum of the α-particles, as measured with a solid-state detector, folded with the resolution of the ionization chamber. The width of the α-line corre-

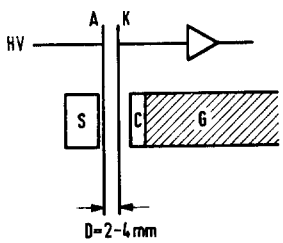

Fig. 1. Experimental set-up to detect β-particles by liquid argon ionization chamber. A anode, K cathode of the chamber, C scintillation detector to detect β-particles, G light-guide, S β-source.

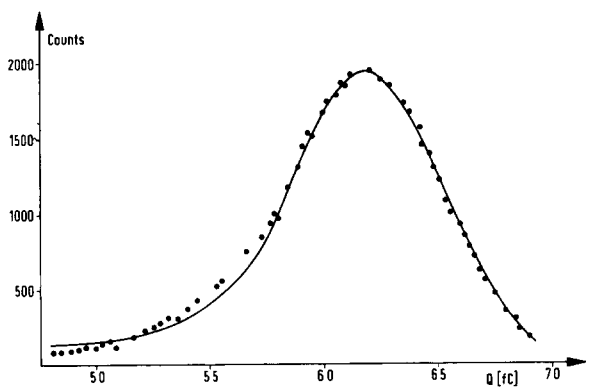

Fig. 2. Energy spectrum of α-particles detected with a liquid argon ionization chamber. Solid line: α-spectrum measured with a solid state detector and folded with the chamber resolution.

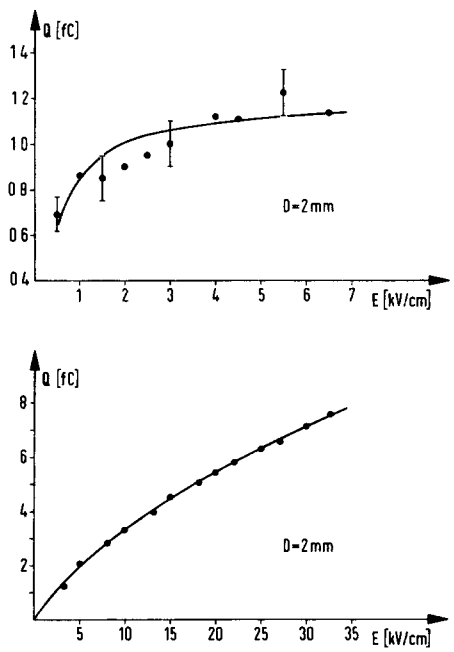

Fig. 3. Charge collected Q as a function of the electric field E between the chamber gaps for a β-source (curve a) and an α-source (curve b) The full curves are theoretical predictions [curve a. eq. (2); curve b eq. (5)]. The concentration of oxygen was $p_{O_2} \lesssim 1$ ppm.

sponds to a charge of 3500 conduction electrons (fwhm), while the number of primary electrons in the ionization column was 2.24×10^5 electrons.

3. Results

3.1. Collected charge

For applications of liquid argon counters the fraction of conduction electrons, produced by the primary particles, which can be detected is of utmost interest. We have measured this number for the cleanest argon available, which had on oxygen contents of less than 1 ppm. For the β-source fig. 3a shows the charge collected as a function of the electric field $|\boldsymbol{E}|$ within the chamber gap. The full curve, included into fig. 3a, is a fit of the theoretical expression[12])

$$Q = Q_0\, 2\,\frac{\lambda}{D}\left[1 - \frac{\lambda}{D}\,(1 - \mathrm{e}^{-D/\lambda})\right] \tag{2}$$

to the data. Q and Q_0 are respectively the detected and the maximum available charge, D is the gap width of the ionization chamber and λ is the mean free path length for the absorption of conduction electrons by impurities (concentration p) in liquid argon. If W is the energy to produce an ion pair in liquid argon, the following relation holds:

$$Q_0 = e\,\frac{\mathrm{d}E}{\mathrm{d}x}\,\frac{D}{W}. \tag{3}$$

The mean free path length λ is assumed to be proportional to the electric field $|\boldsymbol{E}|$ of the chamber gap

$$\lambda = \lambda_0\,|\boldsymbol{E}| = \alpha\,\frac{|\boldsymbol{E}|}{p} = \frac{\tilde{\lambda}}{p}. \tag{4}$$

Q_0 and α are the free parameters in the fit. The results of the fit are given in table 1 for different gap widths D. The proportionality between Q_0 and D is a consistency check for the calibration of the detector. In average $Q_{\max}/Q_0 = (95 \pm 4)\%$ of the total charge produced by the primary β-particles is collected. $Q_{\max}$ is the maximum detected charge. The systematic error of 9% is not included in the error limits given above.

For strongly ionizing α-particles the result differs appreciably (fig. 3b) from that characteristic for β-particles. Even at a field strength of $|\boldsymbol{E}| = 40$ kV/cm no saturation is observed. The maximum fraction of the produced conduction electrons which could be detected was $(25 \pm 3)\%$ at a field strength of 40 kV/cm. Because of discharges, measurements at higher field strengths have not been performed. The full line, included into fig. 3b, is a fit of the expression

$$Q = Q_0\,\frac{\lambda}{D}\,(1 - \mathrm{e}^{-D/\lambda})\,\frac{2f}{\sqrt{\pi}}\int_0^{\infty}\frac{\sqrt{x}}{f\cdot\mathrm{e}^{x}+1}\,\mathrm{d}x, \tag{5}$$

$$f = |\boldsymbol{E}|/|\boldsymbol{E}_0| \tag{6}$$

to the data using eq. (4) for the mean free path length λ. The first term in eq. (5) describes the absorption of conduction electrons by impurities[12]), while the second term was derived by Kramers[13]) to describe the column recombination. $|\boldsymbol{E}_0|$ is the saturation field

Table 1

Maximum detected charge Q_0 produced by β-particles in an ionization chamber with gap width D. The corresponding theoretical value $Q_{0,\mathrm{th}}$ was calculated from $\mathrm{d}E/\mathrm{d}x = 1.9$ MeV/cm[11]) and the energy $W = (23.6 \pm 0.5)$ eV[24]) necessary to produce an ion pair in liquid argon.

D (mm)	Q_0 (fC)	$R = Q_0/Q_{0,\mathrm{th}}$
2	1.20 ± 0.04	0.93 ± 0.05
3	1.90 ± 0.03	0.98 ± 0.04
4	2.43 ± 0.10	0.94 ± 0.05
		$\langle R \rangle = 0.95 \pm 0.04$

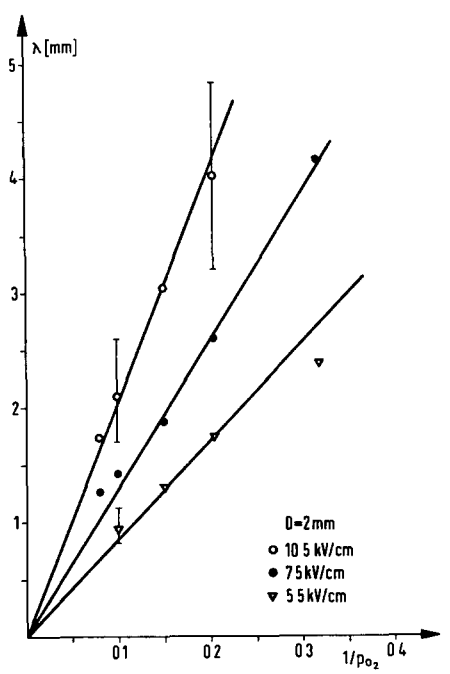

Fig. 4. Mean free path length λ for absorption of conduction electrons produced by a β-source as a function of the oxygen concentration p_{O_2}.

strength of the ionization column, which is given by[13])

$$|E_0| = \frac{4\sqrt{\pi eN}}{b}, \tag{7}$$

(e electric charge, N charge density, b diameter of ionization column). $|E_0|$ was determined by the fit to be $|E_0| = (798 \pm 5)$ kV/cm at a gap width of $D = 2$ mm. For a gap width of the ionization chamber of $D =$ 1.5 mm the saturation field strength $|E_0|$ was systematically lower. No explanation exists for this observation.

3.2. Influence of oxygen and nitrogen impurities on the charge collection

For the β-source the mean free path length λ can be determined from the measured charge Q with the help of eq. (2) and the results for Q_0 given in table 1. Since the ratio Q/Q_0 depends only weakly on the electric field $|E|$ in the plateau region, the mean free path length has its largest error for large $|E|$. At constant electric field $|E|$ the mean free path length λ is proportional to p^{-1} as expected from eq. (4) (fig. 4). For small electric field strengths $|E|$ the linear relationship

$$\lambda \sim |E|,$$

expected to hold if the conduction electrons are thermal, is fulfilled (fig. 5). In this interval we find for the proportionality constant of eq. (4)

$$\alpha = (0.15 \pm 0.03)\,\frac{\text{ppm cm}}{\text{kV/cm}}. \tag{8}$$

For higher field strength $|E| \gtrsim 5$. 10 kV/cm the mean free path length λ rises steeper than linear. The deviation from the linearity eq. (4) seems to start the earlier, the lower the concentration of the impurity (fig. 5).

For nitrogen impurities in the liquid argon we observe practically no absorption, the mean free path length λ_{N_2} for absorption of conduction electrons by nitrogen has a lower limit of

$$\lambda_{N_2} \approx 200\,\lambda_{O_2}. \tag{9}$$

The uncertainty is mainly due to the effect that small concentrations of oxygen in nitrogen can simulate an absorption effect of nitrogen impurities.

For the α-source expression (5) is not as simple as expression (3) for the β-source. In order not to be biased by special assumptions on the recombination effect, we have determined λ from a fit of

$$\frac{Q}{Q_0^*} = \frac{\tilde{\lambda}}{Dp}\,(1 - e^{-pD/\tilde{\lambda}}), \tag{10}$$

(Q_0^* charge at a given $|E|$ extrapolated from $p_{O_2} >$ 10 ppm to $p_{O_2} = 0$ ppm) to the $Q = Q(p)$ curve at constant electric field $|E|$. A typical result is shown in fig. 6. The fit is excellent for $p_{O_2} > 10$ ppm, for smaller concentrations p_{O_2} of the oxygen impurities the experimental data are larger than the prediction of the fit. The results of the analysis are included into fig. 5. Within the error limits there is good agreement between the results of the α-source with those of the β-source. For the constant of eq. (4) we get in case of the α-source

$$\alpha = (0.14 \pm 0.03)\,\frac{\text{ppm cm}}{\text{kV/cm}}. \tag{11}$$

Fig. 7 shows the $Q = Q(p_{N_2})$ dependence for nitrogen

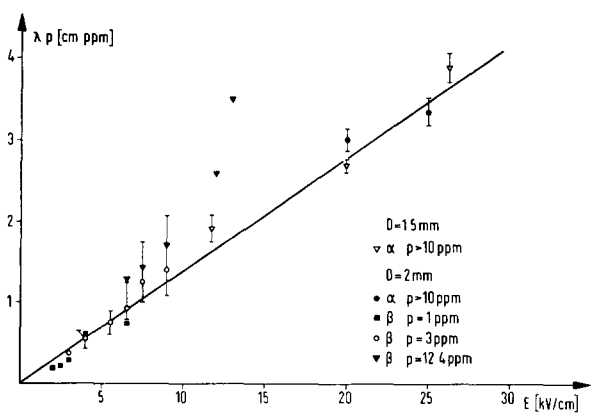

Fig. 5. Mean free path length for absorption λ_{O_2} by oxygen impurities as a function of the electric field $|E|$.

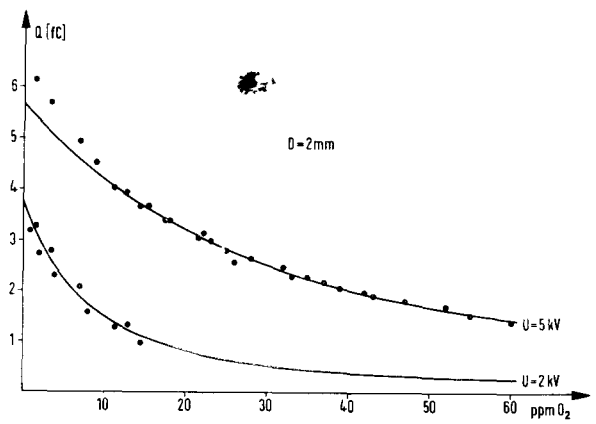

Fig. 6. Charge collected as a function of the oxygen concentration p_{O_2}. The full line is a fit of eq. (10) to the data The conduction electrons were produced by an α-source.

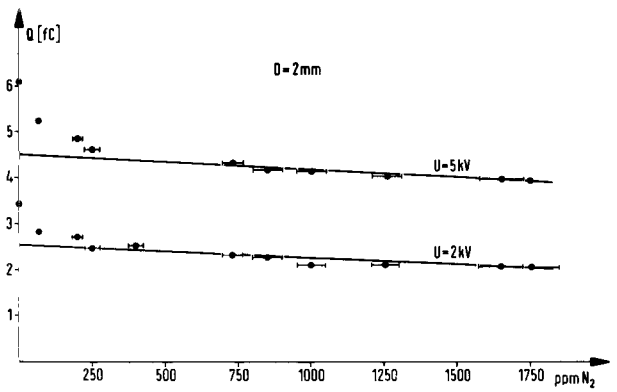

Fig. 7. Same as fig. 6 but for nitrogen impurity concentration p_{N_2}.

impurities. The lower limit eq. (9) for the mean free path length λ_{N_2} derived from the experiment using a β-source is in agreement with the measurements using an α-source. For $p_{N_2} < 250$ ppm deviations of the measured charges Q from the expected ones are observed analogue to the measurements with oxygen impurities. In the case of the β-source these deviations were not observed, therefore this behaviour seems to be characteristic for α-particle ionization columns.

4. Discussion of the results

The fraction of charge collected depends strongly on the ionization density produced by the primary particles and therefore is different for an α-source compared to a β-source (fig. 3). In agreement with the data of Marshall[14]) for a β-source in our experiment $(95 \pm 4)\%$ of the produced conduction electrons are collected. For α-particles no saturation effect is observed in agreement with the observation of previous authors[15–17]). At the maximum possible field strength of 40 kV/cm $(25 \pm 3\%)$ of the produced electrons are detected. This fraction is higher than observed in other experiments. The difference can be explained by polarization effects, which have been avoided in our measurement, while they can not be exlcuded in the foregoing experiments, where point-sources for α-particles were used.

The difference between the results for α- and β-sources is due to the strong recombination effects in the ionization column produced by α-particles. Fig. 3b shows that the recombination in pure liquid argon is quantitatively described by the theory of Kramers[13]). Using the saturation field strength $|\boldsymbol{E}_0|$ determined in the fit and Kramers' theoretical expression given in eq. (7), one gets for the diameter b of the ionization column

$$b = 5 \times 10^{-5} \text{ cm}.$$

This result is in good agreement with the value given by Stacey[18]).

The dependence of the collected charge on the concentration p of the solved impurities shows a deviation from the expected behaviour for the α-source (figs. 6, 7), while for the β-source the theoretical proportionality eq. (4)

$$\lambda \sim p^{-1}$$

holds (fig. 4). This difference demonstrates that the impurities influence strongly the recombination effects in the ionization column produced by α-particles. Indications for this effect have been observed in previous experiments[16,17]) for oxygen impurities. Since the effect is observed already at low field strengths $|\boldsymbol{E}|$ and for quite different concentrations of oxygen ($p_{O_2} < 10$ ppm) and nitrogen ($p_{N_2} < 250$ ppm) it is probably due to three-body recombination effects[20]) and not due to nonthermal conduction electrons[10]).

For small electric fields the mean free path length λ for absorption of conduction electrons by impurities depends linearly on the electric field $|\boldsymbol{E}|$. The value of the proportionality constant α in expression (4) [eqs. (8) and (10)] is in good agreement with the result of Miller et al.[21]).

For higher electric field strengths $|\boldsymbol{E}|$ the mean free path length λ increases steeper than predicted by the linear relationship (4), which holds, if the conduction electrons are thermal. The deviation from the linear relationship (4) between λ and $|\boldsymbol{E}|$ starts at field strengths between $|\boldsymbol{E}| = 5$ kV/cm and 10 kV/cm, depending on the concentration of the impurity (fig. 5). This effect can be explained by the existence of nonthermal hot electrons at higher field strengths. The result is in good agreement with drift velocity measurements[21–23]) and their theoretical interpretation by Lekner[23]). He predicts the thermalization of hot electrons for impurity concentration of $p_{O_2} \gtrsim 10$ ppm in good agreement with the results of the present measurement.

We are grateful to Mr H. Oettinger and W. Schaaf for their help during the construction period. This work was supported by the Bundesministerium für Forschung und Technologie.

References

[1]) C. W. Fabjan, Rapporteur talk, Palermo Conference (1975).
[2]) J. Engler, W. Flauger, B. Gibbard, F. Monnig, K. Runge and H. Schopper, Nucl. Instr. and Meth. **106** (1973) 189.

[3]) W. J. Willis and V Radeka, Nucl Instr. and Meth. **120** (1974) 221.
[4]) J. Engler, B. Friend, W. Hofmann, H. Keim, R. Nickson, W. Schmidt-Parzefall, A. Segar, M. Tyrell, D. Wegener, T. Willard and K. Winter, Nucl. Instr. and Meth. **120** (1974) 157
[5]) G. Knies and D. Neuffer, Nucl. Instr. and Meth. **120** (1974) 1
[6]) C. W Fabjan, W. Struczinski, W. J Willis, C. Kourkoumelis, A J Landford and P. Rehak, Phys. Lett. **B60** (1975) 105.
[7]) J. Engler, W. Hofmann, J. Spengler and D. Wegener, Nucl. Instr. and Meth (in press).
[8]) W. Hofmann, Diplomarbeit (Karlsruhe, 1974) and Kernforschungszentrum Karlsruhe, Externer Bericht 3/74-10 (1974).
[9]) Further details are given in U Klein, Staatsexamensarbeit (Karlsruhe, 1975) (unpublished) and M. Schulz, Staatsexamensarbeit (Karlsruhe, 1975) (unpublished).
[10]) Further details are given in J. Spengler, Diplomarbeit (Karlsruhe, 1975) and Kernforschungszentrum Karlsruhe, Externer Bericht 3/76-2 (1976)
[11]) A. Nelms, National Bureau of Standards, Circular 577
[12]) R. Hilsch and R. W. Pohl, Z. Physik **108** (1937) 55.
[13]) H. A Kramers, Physica **18** (1952) 665.
[14]) J. H. Marshall, Rev. Sci Instr **25** (1954) 232
[15]) A. N. Gerritsen, Physica **14** (1948) 381.
[16]) M. Davidson and A E Larsh, Phys Rev. **77** (1950) 706.
[17]) J Prunier, Thesis (Université de Grenoble, 1973) (unpublished).
[18]) F. D. Stacey, Austr. J Phys **11** (1958) 158.
[19]) D. W. Swan, Proc. Phys Soc **76** (1960) 36.
[20]) J. B. Harted, *Physics of atomic collisions* (Butterworths, London, 1964)
[21]) L. S. Miller, S. Howe and W E Spear, Phys. Rev. **166** (1968) 871.
[22]) H. Schnyders, S. A Rice and L. Meyer, Phys. Rev. **150** (1966) 127.
[23]) J Lekner, Phys. Rev. **158** (1967) 130.
[24]) M Miyajima, T Takahashi, S Konno, T. Hamada, S. Kubota, H. Shibamura and T. Doke, Phys. Rev. **A9** (1974) 1439